Flow Visualization of Two Phase Flow of R245fa in a Microgap with Integrated Staggered Pin Fins

Pouya Asrar [*], Xuchen Zhang, Craig E. Green, Peter A. Kottke, Thomas E. Sarvey, Andrei Fedorov, Muhannad S. Bakir, and Yogendra K. Joshi[*,§]
[*]George W. Woodruff School of Mechanical Engineering, Georgia Institute of Technology, Atlanta, GA 30332, United States
[§]Corresponding author. Fax: +1 404-894-8496 Email: yogendra.joshi@me.gatech.edu

Abstract

We have visualized two phase flow cooling of R245fa refrigerant in a 1 cm x 1 cm x 200 µm microgap, equipped with circular pin-fins. The device has the microgap with sparse circular pin-fin arrangement of transverse pitch, longitudinal pitch, and pin-fin diameter of 225 µm, 225 µm, and 75 µm, respectively. On the back side of the chip, four integrated platinum heaters are fabricated and are arranged in series. The microgap is installed in a closed flow loop that is pressurized. The inlet flow is subcooled at the elevated pressure. Flow boiling is obtained in the microgap for a range of heat flux values between 7 W/cm^2 to 34 W/cm^2. Using a high speed camera, flow visualization results are presented for the range of heat flux values.

Keywords

Two phase flow boiling heat transfer, microfluidic cooling, circular pin fin

Nomenclature

D	Pin Fin hydraulic diameter, µm
D_p	Redistribution line pin fin diameter, µm
H	Microgap height, µm
L	Microgap length, cm
P_L	Longitudinal Pitch, µm
P_T	Longitudinal Pitch, µm
q"	Heat flux, W/cm^2
T_H	Microgap bottom (surface) temperature, ℃
T_{surf}	Microgap bottom (surface) temperature, ℃
W	Microgap width, cm
x	Exit vapor mass quality

1. Introduction

Flow boiling in microchannels and two phase flow visualization has been employed in many applications [1-3]. Yen et al.[4] investigated the visualization of convective flow boiling in two different types of microchannels: square and circular. They found out that the number of nucleation bubbles are more in the square shape microchannel than the circular types. This proved that square microchannel had performed better in terms of heat removal capacity. Different regimes of flow boiling such as bubbly, plug, and annular patterns were observed using a high speed camera. A periodic variation in flow regimes was concluded by the flow visualizations for both square and circular shape channels.

Bogojevic et al.[5] investigated the flow boiling instabilities by looking at bubble dynamics. The microchannel had 40 rectangular channels. They utilized deionized water as the working fluid for mass fluxes ranging between 7-204 kg/m^{2}s. Using a microscope and a high speed camera the effect of heat flux and mass flux on bubble growth was investigated. They categorized the bubbles grown in the microchannel into two different types: bottom wall bubbles and sidewall bubbles. The projected area of bottom wall bubbles and sidewall bubbles were observed to be a circle and a truncated circle, respectively. The diameter of the circle was considered as the reference to determine the bottom wall bubble growth whereas the height of the bubble was measured to be reported as the sidewall bubble growth.

Flow morphologies for a range of mass fluxes were studied by Kuo et al.[6]. They considered 200 µm × 253 µm parallel microchannels for a range of mass flux between 83 kg/m^{2}s to 303 kg/m^{2}s. Bubbly flow was only detected for a limited range of mass velocity of flow. For heat fluxes as high as 53 W/cm^2 the flow was recognized to experience a direct transition from single phase to slug flow.

Flow boiling instabilities of water in 8 microchannels for a range of heat flux and mass were visualized by Wang et al.[7] The microchannels were arranged in parallel, as well as on a single microchannel. For the first experiment, the flows running in each channel had interaction with each other at the header of microchannels.

Isaacs et al.[8] considered a 1×1 cm silicon mircchannel having circular pin fins of 150 µm diameter. They studied the two phase flow of refrigerant R245fa as the working fluid running around a thermal loop. They visualized the flow inside the microgap and were able to identify the vapor nucleation zones. They found out that those locations are strongly dependent on the heat flux range. They observed the triangle-shaped wakes for low heat fluxes and high flow rates towards the end of the microgap.

In the present investigation we demonstrate the use of flow boiling of dielectric refrigerant R245fa as the working fluid running through a microgapl with the dimensions provided in Table 1. The schematic of the microchip is shown on Fig. 1.

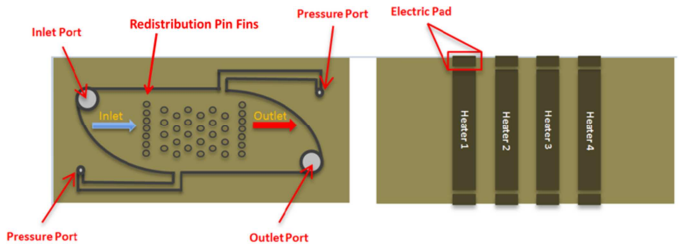

Fig. 1. Chip Schematic

Table 1. Microchannel Dimensions

Microchannel and Pin Fin Arrays Configuration					
D (µm)	P_L (µm)	P_T(µm)	W (mm)	L (mm)	H (µm)
75	225	225	10	10	200
Redistribution Pin Fins Configuration					
D_p (µm)		P_L (µm)		P_T(µm)	
90		20		20	

2. Experimental setup and methods

Figure 2 demonstrates the schematic of the experimental setup. Before charging the system with working fluid, the loop is evacuated using a vacuum pump (VN-200N, JB Industries Inc.). As the next step, the source tank is warmed up to a temperature higher than room temperature to a typical value of 28°C. A 1,000 mL reservoir is then charged with enough refrigerant before charging the rest of the system. In order to guarantee that the syringes are fully charged, the reservoir is heated up to few °C higher than ambient temperature. Continuous flow becomes possible by having one of the pumps infusing, and the other one withdrawing simultaneously. After charging the pumps, the working fluid is pushed by one syringe pump towards the pre-cooler in the system in order to insure its liquid phase. The refrigerant passes through a microturbine flow meter (S-114, McMillan Co.). R245fa is maintained contaminant-free by incorporating a 0.5 µm in-line filter (SS-4F-05, Swagelok Co.). Using a backwash loop in the system, the fluid is run through the chip in both directions for cleaning, prior to running the actual experiment. R245fa finishes the cycle by passing through a heat exchanger (LL510G14, Lytron Co.) before returning back to the 1000 mL reservoir.

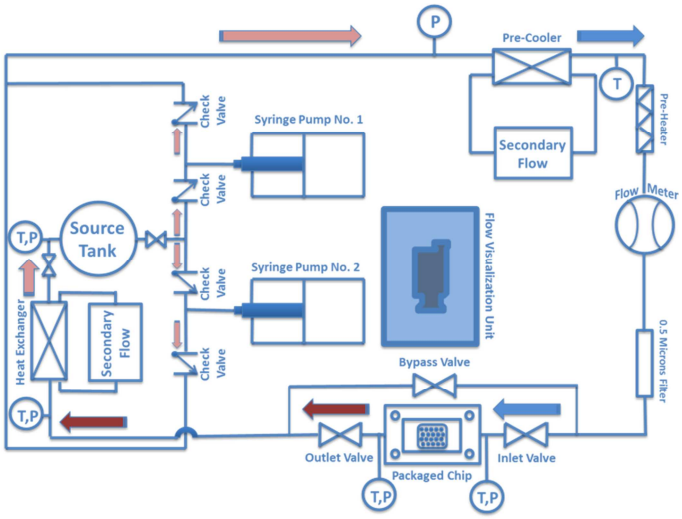

Fig. 2. Flow Loop Schematic

Steady state condition is insured by running the system for a few hours, while recording data such as temperature and pressure values using a data acquisition device. All measured quantities are constant within 0.25% for pressure data and 0.5 °C for temperature data in each pushing cycle under steady state. The heaters are then gradually powered. The voltage and current applied to the heaters are recorded for heat flux calculations. For each heat flux, all measurements are archived.. Flow visualization is performed using a high speed camera (Phantom V211, VISION Research Co.) at 2,229 frames per second.

Figure 3 is the schematic of the test device components prior to assembly. The package made of PEEK has ports designed for inflow and outflow, as well as for pressure and temperature measurements. The device sits in the pocket designed on the back side of the package. Using O-Rings, the ports are sealed. The chip is sealed between a printed circuit board (PCB) and the package. The PCB has electrical pads that are connected to the chip using a wirebonding process. Using two Copper Constantan (T-type) thermocouples 1.56 mm sheath diameter, as well as two pressure transducers, the temperature and pressure data are obtained.

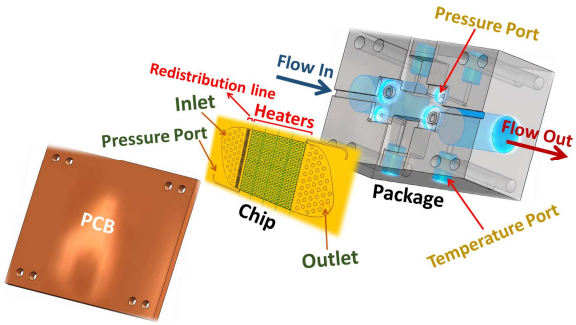

Fig. 3. Test Device Schematic

3. Fabrication process

The microgap consists of a 1 cm x 1 cm array of staggered cylindrical micropin-fins, as shown in figure 4.A. In addition to fluid inlet and outlet ports, pressure ports are included on either side of the micropin-fin array in order to accurately measure pressure drop, while excluding pressure drop due to rapid flow constriction/expansion at the inlet and outlet ports. Four columns of micropin-fins are also introduced upstream of the micropin-fin array, in order to promote a stable and evenly distributed flow. Large mechanical support pins were added near the inlet and outlet for boosting structural strength. Four serpentine platinum heaters/resistance temperature detectors (RTDs) generate heat load and provide temperature measurements in four sections along the flow length (between inlet and outlet).

The process used to fabricate the heat sink testbed is shown in Figure 4.B. Starting with a 500 µm thick double side polished wafer, standard Bosch process was used to create the 200 µm high micropin-fins and manifolds. Next, the cavities formed during etching were sealed using a pyrex cap with anodic bonding at 800 V at 350 °C. The bonded wafer was then flipped over and a 1 µm thick insulating silicon dioxide layer was deposited using chemical vapor deposition (CVD). 200 nm thick Platinum heaters and 500 nm thick gold pads were then deposited on the SiO_2 layer. Another 1 µm thick silicon dioxide passivation layer was deposited on the heater

for protection and thermal isolation. Lastly, inlet, outlet, and pressure measurement ports were etched using Bosch process from the same side of the wafer.

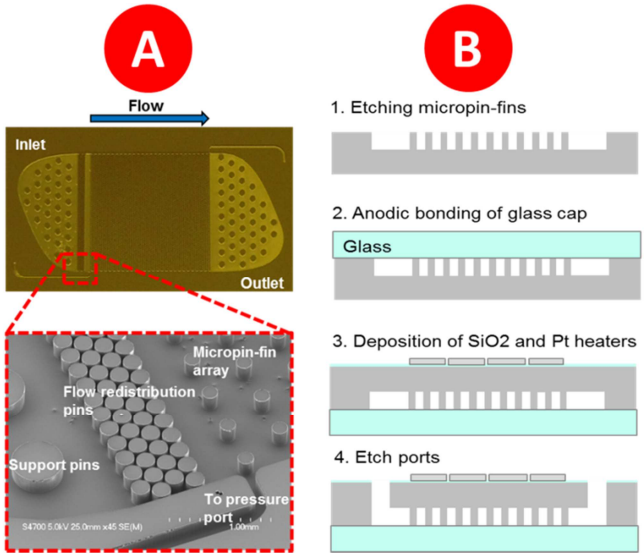

Fig. 4. SEM Picture of the Device (A) and the Fabrication Steps (B)

4. Results and discussion

The flow rate was set to 15 mL/min for all experiments. Starting from a small power (~ 1W) applied to all four heaters; the power was increased gradually until two phase flow was observed in the microgap. The flow boiling first occurred near the exit of the microgap, and upon increasing the heat flux progressed towards the inlet. Table 2 shows a list of maximum heater temperature versus selected heat fluxes. The temperature data are reported considering an uncertainty of 0.5 ℃.

Table 2. Summary of the Experiment Set

Experiment	Heat Flux (W/cm^2)	Max. Wall Temp. (℃)
1	7.72	47 (Heater 4)
2	11.3	54 (Heater 3)
3	15.74	61 (Heater3)
4	25	73 (Heater3)
5	29.2	76 (Heater 3)
6	34	80 (Heater3)

Figure 5 demonstrates the visualizations of the flow boiling for heat fluxes ranging from 11 W/cm^2 to 34 W/cm^2. Two phase flow started via nucleate boiling. Small bubbles were formed around pin-fins in the microgap and grew as they moved to the outlet of the microgap. As shown in figure 5, for heat fluxes of 25W/cm^2 and above, the two phase region is evenly distributed over the microgap. This area progressed more towards the inlet of the chip, as the heat flux increased. The red circles in figure 5 identify the spots where the nucleation was observed around single pin fins. The nucleate boiling occurred at the first column of pin fins of the two phase area in the microgap.

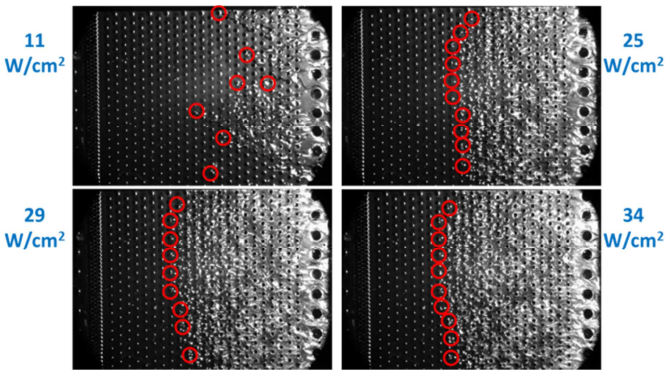

Fig. 5. Flow Visualization Using High Speed Camera

Using a 1D heat conduction calculation, the surface temperature corresponding to each heater temperature was obtained. Figure 6 illustrates the surface temperatures at all four heaters locations on the back of the chip. Heater 4 (closest to the outlet of the chip) showed the maximum surface temperature among all four heaters, whereas for heat fluxes above 25 W/cm^2, heater 3 had the maximum temperature.

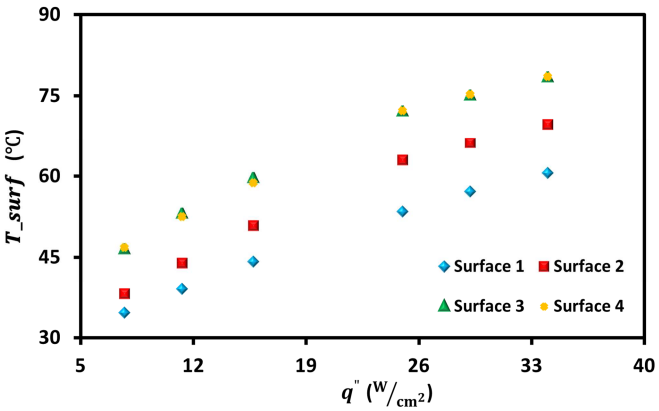

Fig. 6. Surface Temperature Distribution

Figure 7 demonstrates the visualization results related to 11 W/cm^2 heat flux in more detail. Figure 7A clearly shows the triangle-shaped two phase wakes covering a few spots downstream of the pin fin array. This wake structure demonstrates the rapid downstream spreading of bubbles generated around pin fins, as also observed by Isaacs et al.[8]. Figure 7.B illustrates the flow boiling of a particular part of the gap at two different time frames. The first picture relates to the initiation of the bubbles around the pin fins, whereas the second clearly shows that a larger volume of vapor has covered the pin fins in the microgap, because of evolution of two phase region with respect to time.

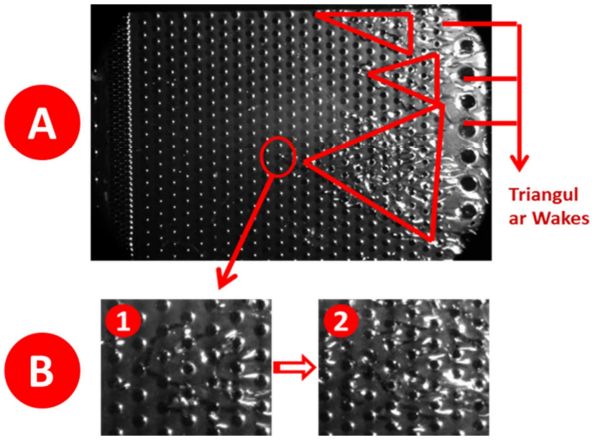

Fig. 7. Triangle-Shaped Liquid/Vapor Wakes Happening at 11 W/cm^2 (A), Close-Up at the Nucleation Zone (B)

Thermodynamic quality of vapor in the boiling region is represented in figure 8. The maximum quality of ~30% was calculated at the maximum heat flux of 34 W/cm^2 .

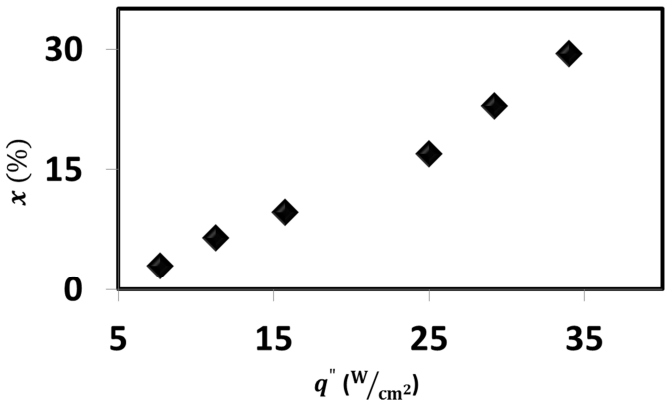

Fig. 8. Vapor Quality Distribution

At higherheat fluxes, the outlet fluid temperature rises correspondingly. The maximum temperature of 60 ℃ was recorded by the thermocouple located near the outlet of the chip. The outlet chip temperature distribution is illustrated by figure 9.

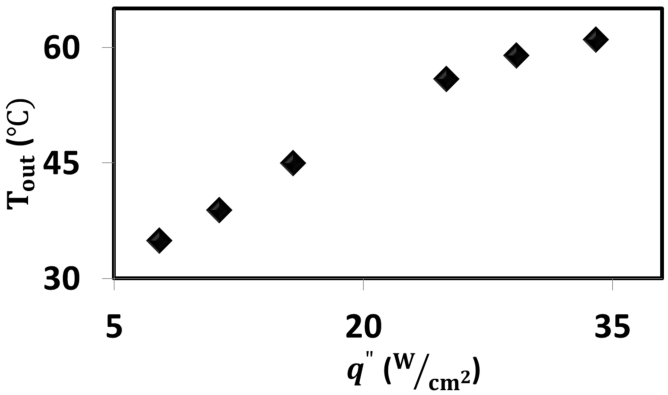

Fig. 9. Fluid Outlet Temperature Distribution

5. Conclusions

A simultaneous visualization and thermal measurement study was done on two phase flow of refrigerant R245fa in a test device having a microgap equipped with circular pin fins. The heat flux ranged from 7 W/cm^2 to 34 W/cm^2. The nucleation zones around individual pin fins were observed via flow visualizations recorded using a high speed camera. A maximum vapor quality of about 30% was calculated at the outlet of the test device.

Acknowledgments

The authors thank the DARPA IceCool Fundamentals Program for providing the financial support for this research.

References

1. D. Bogojevic, K. Sefiane, A.J. Walton, H. Lin, G. Cummins, D.B.R. Kenning, T.G. Karayiannis, “Experimental investigation of non-uniform heating effect on flow boiling instabilities in a microchannel-based heat sink”, International Journal of Thermal Sciences Vol. 50, pp. 309-324, 2010.
2. Chun Ting Lu and Chin Pan, “A highly stable microchannel heat sink for convective boiling”, Journal of Micromechanics and Microengineering, Vol. 19, No. 5, p. 055013, 2009.
3. Ayman Megahed, “Experimental investigation of flow boiling characteristics in a cross-linked microchannel heat sink”, International Journal of Multiphase Flow, Vol. 37, pp. 380-393, 2010.
4. Tzu-Hsiang Yen, Masahiro Shoji, Fumio Takemura, Yuji Suzuki, Nobuhide Kasagi. “Visualization of convective boiling heat transfer in single microchannels with different shaped cross-sections”, International Journal of Heat and Mass Transfer, Vol. 49, pp. 3884-3894, 2006.
5. D. Bogojevic, K. Sefiane, G. Duursma, A.J. Walton, “Bubble dynamics and flow boiling instabilities in microchannels”, International Journal of Heat and Mass Transfer, Vol. 58, pp. 663-675, 2013.
6. C.-J. Kuo, Y. Peles, “Local measurement of flow boiling in structured surface microchannels”, International Journal of Heat and Mass Transfer, Vol. 50, pp. 4513-4526, 2007.
7. Guodong Wang, Ping Cheng, Huiying Wu, “Unstable and stable flow boiling in parallel microchannels and in a single microchannel”, International Journal of Heat and Mass Transfer, pp. 4297-4310, 2007.
8. Steven A. Isaacs, Yoon Jo Kim, Andrew J. McNamara, Yogendra Joshi, Yue Zhang, Muhannad S. Bakir, “Two-Phase Flow and Heat Transfer in Pin-Fin Enhanced Micro-Gaps”, 13th IEEE InterSociety Conference on Thermal Phenomena in Electronic Systems, pp. 1084-1089, 2012.